Available online at www.sciencedirect.com
SCIENCE DIRECT®
Journal of Pharmaceutical and Biomedical Analysis
32 (2003) 401–408
JOURNAL OF PHARMACEUTICAL AND BIOMEDICAL ANALYSIS
www.elsevier.com/locate/jpba

Modeling the effect of analyte and reference bandwidths on signal and noise magnitudes in spectrophotometric assays

C. Galli [a,*], P.J. Frey [b], P. Harmon [b], H. Hartman [b], R.A. Reed [b]

[a] *Pfizer Global Research and Development, Pharmaceutical Sciences-Ann Arbor, 2800 Plymouth Road, Ann Arbor, MI 48105, USA*
[b] *Pharmaceutical Analysis and Control, Merck Research Laboratories, WP 78-110, PO Box 4, West Point, PA 19486, USA*

Received 8 April 2002; received in revised form 14 February 2003; accepted 20 February 2003

Abstract

In spectrophotometric assays, it has been well established that the recorded absorption, and therefore the experimentally determined extinction coefficient, decreases as a function of detected bandwidth. This manuscript presents an expression for the extinction coefficient as a function of the critical parameter detected bandwidth per transition linewidth. Calculations for both single channel and multichannel photodetection are presented; the derived expressions are shown to be in good agreement with experimental results. It is important to realize that this systematic bias is present in dilute solutions of low absorptivity, and the experimentally recorded extinction coefficient for a molecular standard such as caffeine can vary approximately 4% or more, depending upon choice of research instrumentation. The magnitude of this bias may be sufficient to effect method robustness, cause interlaboratory discrepancies, and fail system suitability requirements for spectrophotometric assays. The signal to noise ratio, for example as analyzed in HPLC/UV–VIS detected chromatograms, is also a function of the detected bandwidths of both the analyte and reference channels. It is shown here that use of a reference can only increase the baseline noise.

Keywords: Beer's Law deviation; Detected bandwidth; Method transfer; Method robustness; Extinction coefficient

1. Introduction

Analytical quantitation via spectrophotometric assay is ubiquitous in research and development environments. Spectrophotometric data can be rapidly acquired, with high precision, even by lab personnel without extensive training. In addition, the required spectrophotometric equipment can be relatively inexpensive, portable, and rugged, facilitating spectral examination of processes as well as products. But analyte quantitation via absorption measurement dominates analytical methodology primarily because the Beer–Lambert law, also known as Beer's Law [1], provides a simple

* Corresponding author. Tel.: +1-734-622-4323; fax: +1-734-622-7711.
E-mail address: christopher.galli@pfizer.com (C. Galli).

0731-7085/03/$ - see front matter
doi:10.1016/S0731-7085(03)00154-7

algebraic expression relating the recorded electromagnetic power of the assay beam to the concentration of the analyte. Typically, the analyte quantitation can be performed using a single standard and the Beer–Lambert law, without additional inputs such as scattering corrections or medium refractive index. Although the effect of the detected spectral width on absorption measurements has been well established in the optical literature for over 70 years [2–8], the quantitative effect of this experimental parameter typically does not receive sufficient attention. In a previous paper [8], a model was generated to calculate the systematic inaccuracies in spectrophotometric assays as a function of analyte concentration and the change in the molecular extinction coefficient over the spectral width of the assay beam. It is hoped the quantitative model presented here, which describes absorption or experimental extinction coefficient as a function of the critical parameter detected spectral width per transition width, will similarly aid in developing robust methods and assigning cause to interlaboratory discrepancies.

Developers of spectrophotometric analytical methods take great care to characterize the relationship between the absorptive response and diluent properties such as pH, solvent polarity, and ionic strength. For assays employing separation prior to data acquisition, the mobile phase may require similar scrutiny. This attention to detail must be particularly ardent for spectrophotometric methods which are developed for subsequent use in a range of research and manufacturing settings, i.e. a method that is transferred. However, the physical components of the Beer–Lambert law are not always examined with sufficient rigor by scientists developing a spectrophotometric protocol or method.

Failure to appreciate the Beer–Lambert law as accurate only in the limit of zero analyte concentration and infinitely monochromatic light may allow interlaboratory discrepancies to resist assignable cause. Measuring the absorbance linearity as a function of analyte concentration allows careful analysts to determine the experimental regime in which the optical properties of the system respond as a Beer–Lambert system. Typically, a nonlinearity due to increased analyte concentration results from nonexponential power decay of the assay beam over the optical path in the sample, the samples are known as ''optically thick''.

However, the quantitative effect of a polychromatic assay beam typically does not receive such critical evaluation [8]. To alert measurement scientists to the functional dependence of the experimentally recorded absorbance on the detected spectral width, commonly referred to as bandwidth, this paper models the magnitude of the (absorption) signal and noise as a function of the experimentally chosen bandwidth. It is important to realize the absorbance signal, and therefore, the experimentally determined molecular extinction coefficient, can vary by approximately 4% depending upon the choice of commercial instrumentation. This systematic bias is present in ''flat'' regions of the absorbance spectrum (e.g. at the peak of a molecular transition = $\text{lambda}_{\text{max}}$), is independent of nonlinear Beer–Lambert behavior due to optically thick samples, and is observed in dilute solutions of low absorptivity.

Below, two models are developed: (1) the single channel model expresses the absorption (or extinction coefficient) as a function of the detected spectral width for experimental devices which employ a single photodetector, and (2) the multichannel model expresses the absorption (or extinction coefficient) as a function of the detected spectral width for spectrophotometers which employ a photodiode array. Noise magnitudes as a function of detected bandwidth are then analyzed, allowing examination of signal-to-noise (S/η) issues. Finally, the effect of the reference channel on S/η is examined.

2. Theory

2.1. Derivation of model: absorption as a function of detected spectral width

An expression for chromatographic absorption recorded by devices employing a single photodetector can be derived from the transmission T_{SC} [7,8]:

$$T_{SC}(\tau) = \frac{\int_0^\infty d\omega \Pi_0(\omega - \omega_0; \Gamma_S) 10^{-\varepsilon(\omega-\omega_m;\Gamma_m)c(\tau)l}}{\int_0^\infty d\omega \Pi_0(\omega - \omega_0; \Gamma_S)}, \quad (1)$$

where ω is the optical frequency of the assay radiation, and Π_0 is the power of the assay probe beam. The power of the probe beam $\Pi_0(\omega - \omega_0; \Gamma_S)$ is Gaussian with respect to the optical frequency components ω, is centered at the optical frequency component ω_0, and has a spectral width (full width at half maximum, FWHM) of Γ_s. The electronic transition of the analyte is described by the decadic extinction coefficient ε. The electronic transition function $\varepsilon(\omega - \omega_m; \Gamma_m)$ is Gaussian with respect to the optical frequency components ω, is centered at ω_m, and has a transition linewidth of Γ_m (FWHM). The concentration of the analyte at the detector is c(τ), the retention time is τ, and the optical path length is *l*. Eq. (1) can be interpreted as the transmission averaged with respect to wavelength over the detected spectral width; the Gaussian probe beam Π_0 weighs the value of the transmission $10^{-\varepsilon cl}$, the expression is then normalized by dividing by the total weight.

For most laboratory situations, the exponent in Eq. (1) is much less than 1, and can be expanded in a Maclaurin series and truncated after the second term ($10^{-x} \approx 1 - x$). An expression for Absorption_{SC}, the single channel absorption when the analyte concentration is changing slowly with respect to the sampling frequency (e.g. static UV assay or a noninstrument limited chromatographic peak), is obtained by direct integration of Eq. (1):

$$\text{Absorption}_{SC} = (1 + b)^{-\frac{1}{2}} l c_0 \varepsilon_m e^{-\frac{4(\ln 2)\Delta\omega^2}{\Gamma_m^2(1+b)}} \quad (2)$$

where $b = (\Gamma_s/\Gamma_m)^2$, c_0 is the analyte concentration, ε_m is the molecular extinction coefficient at ω_m, and $\Delta\omega^2 = (\omega_0 - \omega_m)^2$. Note as $b \to 0$, the Beer–Lambert expression for an infinitely monochromatic assay beam is recovered. Because the extinction coefficient $\varepsilon(\omega - \omega_m)$ was modeled as a Gaussian in Eq. (1), the magnitude of the absorption signal (Eq. (2)) displays Gaussian decay with respect to the detuning Δω. Experimentally the parameter Δω, which expresses the detuning from the absorption maximum, can have any value chosen by the analyst. There are two values for Δω, which are particularly instructive. For the first value of interest, $\Delta\omega = 0$ (i.e. $\omega_0 = \omega_m$), Eq. (2) is plotted as a solid line in Fig. 1A; the figure is captioned lambda_{max}. For the second value of interest, $\Delta\omega = \Gamma_m/2$, Eq. (2) is plotted as a solid line in Fig. 1B; the figure is captioned $\text{lambda}_{halfmax}$.

Spectrophotometers employing multichannel detection elements, such as a photodiode array detector interfaced with a chromatographic module, calculate absorption using the instrument software to combine diode responses. Consider a slit width of σ, such that each detector element *i* in the array records over a Gaussian spectral width of σ nm. The transmission calculated from an array of detectors can be expressed:

$$T_{MC}(\tau) = N^{-1} \sum_i^N \times \frac{\int_0^\infty d\omega \Pi_i(\omega - \omega_i; \sigma) 10^{-\varepsilon(\omega-\omega_m;\Gamma_m)c(\tau)l}}{\int_0^\infty d\omega \Pi_i(\omega - \omega_i; \sigma)} \quad (3)$$

where Π_i is the (Gaussian) probe beam of spectral width σ, centered at optical frequency ω_i. Following the MacLaurin expansion of the exponent in Eq. (3), the absorption is then calculated by direct integration:

$$\text{Absorption}_{MC} = N^{-1} \sum_i^N (1 + \beta)^{-\frac{1}{2}} l c_0 \varepsilon_m e^{-\frac{4(\ln 2)\Delta\omega_i^2}{\Gamma_m^2(1+\beta)}} \quad (4)$$

where N is the number of detectors employed for the absorbance calculation, $\beta = (\sigma/\Gamma_m)^2$, and $\Delta\omega_i^2 = (\omega_i - \omega_m)^2$. As $\beta \to 0$, the Beer–Lambert limit is recovered. For the experimental situation in which absorption maximum is chosen as the detection wavelength, i.e. $\Delta\omega = 0$, Eq. (4) is plotted

as a dotted line in Fig. 1A; the figure is captioned lambda$_{max}$. For the experimental situation in which the detection setting is such that $\omega_0 = \omega_m + \Gamma_m$, i.e. $\Delta\omega = \Gamma_m/2$, Eq. (4) is plotted as a dotted line in Fig. 1B; the figure is captioned lambda$_{halfmax}$. The numerical difference between Eqs. (2) and (4), the two absorption models, is relatively slight; for practical estimations of ab-

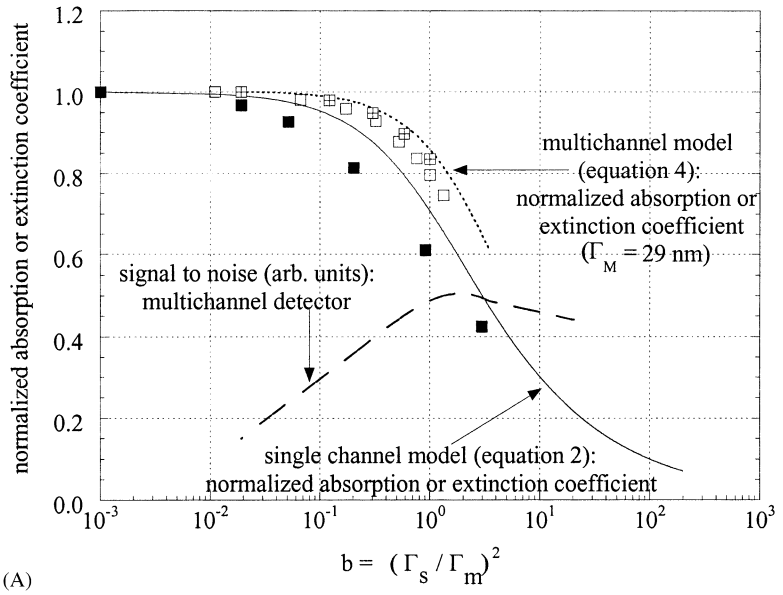

(A)

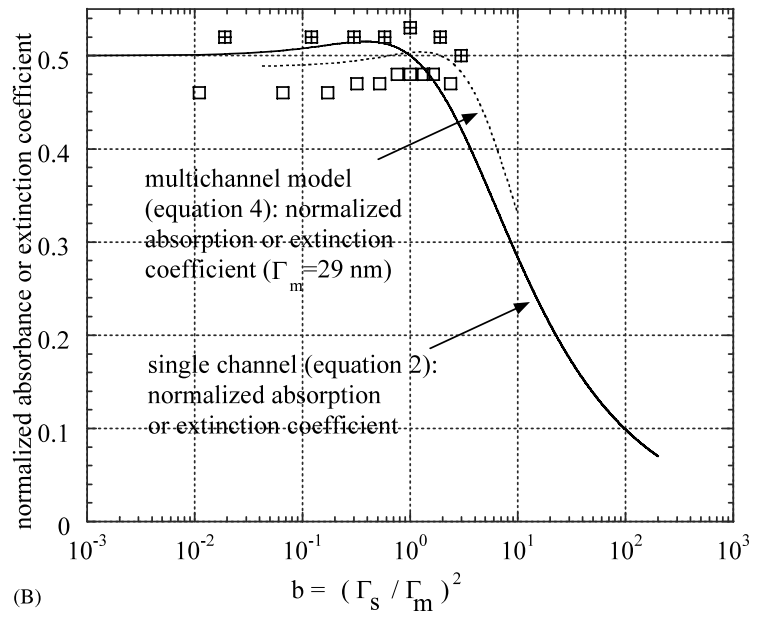

(B)

Fig. 1.

sorption diminution as a function of detected bandwidth, the more tractable expression Eq. (2) serves well.

The solid line in Fig. 1A is Eq. (2) evaluated at the maximum optical response of the analyte (i.e. lambda_{max}). As expected, the function decreases monotonically; the experimentally determined molecular extinction coefficient can only decrease as the bandwidth is widened to include wavelengths of lower optical response. For $b = 1$, the detected bandwidth extends to wavelengths of one-half the maximum optical response, so a sensible estimate for a measurement of the molecular extinction coefficient with these conditions would be approximately 75% of the true value: $((1+0.5)/2 = 0.75)$. Note the value of Eq. (2) at $b = 1$ is $2^{1/2}(= 0.71)$. The solid line in Fig. 1B is Eq. (2) evaluated at a detection wavelength of one-half the maximum optical response (detection setting $\omega_0 = \omega_m + \Gamma_m/2 \equiv \text{lambda}_{halfmax}$). With this detection setting, the function is fairly constant through $b = 1$; the smaller absorbance recorded at wavelengths of lower optical response is offset by the larger absorbance recorded at wavelengths of larger optical response. For $b > 1$, the function decreases monotonically as the optical response is everywhere decreasing for wavelengths in this spectral range.

3. Experimental

3.1. Signal magnitude as a function of detected spectral width

For comparisons between experimental values and Eq. (2), the Pr^{+3} absorption data presented by Wentworth [7] was analyzed and plotted in Fig. 1A (solid squares; $\text{lambda}_{max} = 589$ nm). Although the absorption lineshape is only roughly Gaussian, and the experimental absorption (or molecular extinction coefficient) is consistently lower than predicted by Eq. (2), the agreement between theory and experiment is, for this example, good (within 10%).

For comparison between experimental values and Eq. (4), HPLC chromatograms of caffeine and sorbic acid were acquired on a multiwavelength detector as a function of user-entered bandwidth, with slit settings (σ) of 4 nm, and method concentrations of 0.1 and 0.01 mg/ml (HP 1100 series diode array detector DAD, Hewlett–Pack-

Fig. 1. (A) Solid line: single photodetector model (Eq. (2)) evaluated at lambda_{max}. Dotted line: multichannel photodetector model (Eq. (4)) evaluated at lambda_{max}. Dashed line: signal to noise curve calculated in text. Solid squares: experimental results of Pr^{+3} absorbance using single photodetector (from Wentworth [7]); normalized absorption at lambda_{max} plotted as a function of $b = (\Gamma_S/\Gamma_m)^2$. Caffeine (hatched squares) and sorbic acid (open squares) peak maximums: HPLC/UV assay results at lambda_{max} using HP DAD 1100 detector array. Chromatographic conditions: caffeine: 0.1 mg/ml concentration; Keystone Scientific Hypersil C18, 5 μm, 150 × 4.6 mm column; 24 °C column temperature; 1.0 ml/min flow; 19.5 μl injection; mobile phase: 40:60 methanol:water; diluent: 30:70 methanol:water. 272 nm detection wavelength; 4 nm slit width; $\Gamma_m = 29$ nm (mean of width determined by fitting absorption spectrum to Gaussian and graphical width determination). Sorbic acid: 0.05 mg/ml concentration; Zorbax RX-C8, 150 × 4.6 mm column; 24 °C column temperature; 1.5 ml/min flow; 26.0 μl injection; mobile phase: 83:17 80 mM $NaH_2PO_4 \cdot H_2O_{(aq)}$ pH 2.9:ACN; diluent: 25:75 methanol:0.13 N aqueous HCl. 263 nm detection; 4 nm slit width; $\Gamma_m = 39$ nm (absorption width determined graphically). Note: The numeric value of the multichannel photodetector model (Eq. (4)) has a very weak dependence on Γ_m. Eq. (4) evaluated at $b = 1$, $\Gamma_m = 29$ nm divided by Eq. (4) evaluated at $b = 1$, $\Gamma_m = 39$ nm is 1.01, i.e. agree within 1%. For plotting Eq. (4) in A and B, Γ_m was set equal to 29 nm. (B): Solid line: single photodetector model (Eq. (2)) evaluated at $\text{lambda}_{halfmax}$. Dotted line: multichannel photodetector model (Eq. (4)) evaluated at $\text{lambda}_{halfmax}$. Caffeine (hatched squares) and sorbic acid (open squares) peak heights: HPLC/UV assay results at $\text{lambda}_{halfmax}$ using HP DAD 1100 detector array. Chromatographic conditions: caffeine: 0.1 mg/ml concentration; Keystone Scientific Hypersil C18, 5 μm, 150 × 4.6 mm column; 24 °C column temperature; 1.0 ml/min flow; 19.5 μl injection; mobile phase: 40:60 methanol:water; diluent: 30:70 methanol:water. 287 nm detection; 4 nm slit width; $\Gamma_m = 29$ nm. Sorbic acid: 0.05 mg/ml concentration; Zorbax RX-C8, 150 × 4.6 mm column; 24 °C column temperature; 1.5 ml/min flow; 26.0 μl injection; mobile phase: 83:17 80 mM $NaH_2PO_4 \cdot H_2O_{(aq)}$ pH 2.9:ACN; diluent: 25:75 methanol:0.13 N aqueous HCl. 282 nm detection; 4 nm slit width; $\Gamma_m = 39$ nm.

ard, Waldbronn, Germany). The resulting peak heights under these conditions were approximately 900 and 90 mV corresponding to the injected concentration (1 V = 1 Absorbance unit). As there was no correlation observed between diminution of absorbance with respect to the detected spectral width and absolute peak height, only the data for the nominal peak height 900 mV is presented; these experimental conditions are the most representative of routine assay work. For chromatograms recorded with the detection wavelength set to lambda_{max}, the results are plotted in Fig. 1A; results for those acquired at $\text{lambda}_{halfmax}$ are plotted in Fig. 1B (complete experimental conditions are given in the figure captions). The agreement between the experimental and theoretical results are good: as predicted by the lambda_{max} diode array detector model (dotted line, Fig. 1A) the HPLC/UV results for both caffeine and sorbic acid are well above the single channel model (solid line, Fig. 1A). Because of the spectral overlap in the multichannel detection scheme, in which wavelengths of high optical response contribute significantly to a number of adjacent detectors, the multichannel detector experimental results and theoretical model (Eq. (4)), lie above the single channel experimental results and theoretical model (Eq. (2)), for all values of Γ_S/Γ_m. This diode array weighting scheme for the absorbance calculation causes the multichannel detection to decline less rapidly with respect to b than the single channel detection.

Applicable data for $b > 1$ is not available for caffeine or sorbic acid, as the optical transitions centered at 272 nm (caffeine) and 263 nm (sorbic acid) are not sufficiently isolated from more energetic transitions. For this reason, and the decrease in multichannel signal to noise for $b > 2^{1/2}$ (discussed below), the diode array detector model was not calculated past $b = 3$.

For a nonchromatographic example, consider the following: a spectrophotometric method developed on an Agilent HP8453 spectrophotometer, $\Gamma_S = 1$ nm, results in an extinction coefficient system suitability requirement of 37.93 ml/mg cm ± 1.5%, for the standard at lambda_{max} (Agilent Technologies, Hewlett-Packard). Let the spectrophotometric accuracy for this spectrophotometer, as well as for a Beckman-Coulter DU®Series 500, $\Gamma_S = 5$ nm, and a Thermo Spectronic®20+, $\Gamma_S = 20$ nm, be < 1e-3 absorbance units. For the solution yielding an extinction coefficient of 37.93 ml/mg cm on the Agilent HP8453, Eq. (2) predicts the Beckman-Coulter DU®Series 500 result will be 37.22 ml/mg cm, and the ThermoSpectronic®20+ will be 29.66 ml/mg cm (molecular FWHM Γ_m = 25 nm, detection at lambda_{max}). The extinction coefficients measured on the latter two spectrophotometers deviate from the extinction coefficients measured on the Agilent HP8453 by 1.9 and 21.8%, respectively, and are considered unacceptable (i.e. > 1.5% deviation), not because of any inaccuracy or error, but because the spectrophotometers performed to their specifications.

3.2. Noise magnitude as a function of detected spectral width

Noise in chromatograms employing absorption detection has contributions from both the analyte channel, which is the photodetector recording the probe beam attenuated by molecular absorbance, and the reference channel, which is the photodetector recording the power of the unattenuated probe beam. The reference detector may sample the probe beam power prior to the sample cell (as in a TSP 1000-3000, Thermo Separation Products, Riviera Beach, FL), or, in multiwavelength detectors, at a wavelength selected by the analyst, presumably where no eluting species absorbs light, (as in a HP DAD 1100; DAD ≡ diode array detector). Recording both the analyte and reference photoresponses allows calculation and presentation of the data as Beer–Lambert absorbance.

Signal to noise (S/η) values and detection limits in chromatograms are typically determined by statistical analysis of the data points in the "baseline", i.e. a region of the chromatogram which has no evidence of analyte elution. The data point at retention time τ constitutes the signal $S(\tau)$, and is calculated from the analyte and reference responses:

$$S(\tau) = \log_{10}\langle V_A\rangle(\tau) - \log_{10}\langle V_R\rangle(\tau) \quad (5)$$

where V_A is the photovoltage at the analyte detector, and V_R is the photovoltage at the reference detector. The brackets indicate an average over the time constant of the photocircuit, and in the case of a multiwavelength detector array, an average over the N detectors employed in the absorbance calculation. The scatter in the data points $S(\tau_i)$, $S(\tau_j)$, $S(\tau_k)\ldots$, which is statistically analyzed to determine the limits of detection, arises from the propagation of the uncertainties in the average quantities $\langle V_A \rangle$ and $\langle V_R \rangle$, and can be expressed via propagation of error formalism [9]:

$$\Delta_{ABS} = \left(\left(\frac{\Delta_{\langle V_A \rangle}}{\langle V_A \rangle} \right)^2 + \left(\frac{\Delta_{\langle V_R \rangle}}{\langle V_R \rangle} \right)^2 \right)^{\frac{1}{2}} = \left(\left(\frac{s_A(N)}{\langle V_A \rangle} \right)^2 + \left(\frac{s_R(N)}{\langle V_R \rangle} \right)^2 \right)^{\frac{1}{2}} \quad (6)$$

where Δ_{ABS} is the uncertainty in absorption, $\Delta_{\langle VA \rangle}$ is the uncertainty in $\langle V_A \rangle$, and $\Delta_{\langle VR \rangle}$ is the uncertainty in $\langle V_R \rangle$. In Eq. (6), this uncertainty is equated with the (estimated) standard deviation s. For single channel detection, $s_{A\ or\ R}$ expresses the (voltage) width of stochastic events in the photocircuit. For multichannel detection, the value of $s_{A\ or\ R}$ can be reduced by averaging $V_{A\ or\ R}$ over N photodetectors, each centered at a unique wavelength; for this reason, s in Eq. (6) is written as an explicit function of N. As averaging over N photodetectors is equivalent to making N independent measurements of $V_{A\ or\ R}$, the standard deviation $s_{A\ or\ R}$ is expected to decrease as $N^{1/2}$. This was experimentally verified by recording chromatograms of caffeine and sorbic acid as a function of Γ_S, graphically measuring the scatter in the baseline, and plotting the scatter verses $N^{1/2}$ (data not shown; reference set to *off* as discussed below). The resulting plots were satisfactorily linear (linear correlation coefficient > 0.98).

Given the functional dependance of both the multichannel absorbance signal (Eq. (4)), and the noise η (i.e. η proportional to $N^{-1/2}$), the signal to noise as a function of detected spectral width is calculated and plotted as a dashed line in Fig. 1A. The signal to noise function increases sharply for b up to $b = 2^{1/2}$, then begins a gradual decline, as further increase in detected spectral width adds little signal.

3.3. Role of reference channel in noise magnitudes

With the availability of digital memory, it is possible to calculate the "absorbance" value at any time τ_j without sampling the reference photovoltage. For example, the photovoltage in the analyte channel at time τ_0 can be written into memory, then used in place of the reference photovoltage at time τ_j (Eq. (5)) for the "absorption" calculations for data points $S(\tau_j)$, $S(\tau_k)$, etc. In the software which controls the HP 1100 DAD (HP ChemStation for LC, Rev. A.06.04 [509]), the user may choose to record a UV–VIS detected chromatogram in this manner by setting the reference to *off*. A consequence of this method of data acquisition is the absorbance value then has but one noise component, $\Delta_{\langle VA \rangle}$ (Eq. (6)). In the limit that the two uncertainty components listed in Eq. (6) are approximately equal, data acquired in the absence of a reference photovoltage should display, by a factor of $2^{1/2}$, a reduction in the "fast" baseline noise, i.e. in the frequency regime of the data acquisition rate. Graphical or statistical analysis of this fast baseline noise is a typical approach to determine the limit of detection of a given chromatographic method.

To measure the contribution of the reference channel to a method limit of detection, successive chromatograms were acquired first with the reference set to *off*, then with the reference bandwidth set to the analyte bandwidth (slit = 4 nm, analyte bandwidth = 4 nm, reference bandwidth = 4 nm). While the chromatograms recorded with the reference set to *off* did have a higher signal to noise than those employing the reference described above, the improvement was slightly less than $2^{1/2}$. Recalling that the analyte and reference channels have different spectral locations, perhaps the lamp fluctuation spectra in these regions differ. It should also be noted that the (less than) $2^{1/2}$ signal to noise improvement upon setting the reference to *off* may be small compared with the attenuation of mobile phase pump oscillations gained for references traversing the chromatographic flow cell.

4. Conclusion

This manuscript has presented a novel, quantitative expression for the experimental molecular extinction coefficient or absorption value as a function of detected spectral width for both single channel and multichannel detection. The critical parameter for this functional dependance has been identified as the detected spectral width Γ_S per molecular transition width Γ_m. The dependence of the experimental absorption or molecular extinction coefficient on (Γ_S/Γ_m) is present in samples of low absorptivity, and may be responsible for method transfer failures and interlaboratory discrepancies. Failure to understand the effect of concentration [8] or detected spectral width [1–8] on the Beer–Lambert absorption law can result in unassigned interlaboratory discrepancies and method transfer failures; it is hoped this manuscript contributes to the development of robust spectrophotometric assays.

Acknowledgements

The corresponding author would like to thank Steve Biffar and Andreas Abend, of Merck Research Laboratories, West Point, PA, for fruitful discussions.

References

[1] H.K. Hughes, Anal. Chem. 24 (1952) 1349–1355.
[2] V. Kondraft'ev, J. Russ. Phys.-Chem. Soc. Phys. Pt. 62 (1930) 153–158.
[3] E. Rottmann, Acta Histochem. 1 (1954) 97–110.
[4] H. Goldenberg, Anal. Chem. 26 (1954) 690–693.
[5] L. Riccoboni, Met Ital. 52 (6) (1960) 289–305.
[6] V.P. Bakhanov, E.R. Tsipkin, Pratsi Odes'k University, Prirodn. Nauki. 152 (8) (1962) 46–50.
[7] W. Wentworth, J. Chem. Educ. 43 (1966) 262–264.
[8] C. Galli, J. Pharm. Biomed. Anal. 25 (2001) 803–809.
[9] D.P. Shoemaker, C.W. Garland, J.W. Nibler, Experiments in Physical Chemistry, McGraw-Hill, New York, 1996, pp. 55–61.